

CALCULATION OF FEYNMAN DIAGRAMS WITH ZERO MASS THRESHOLD FROM THEIR SMALL MOMENTUM EXPANSION

J. FLEISCHER^{a1}, V.A. SMIRNOV^{b2} and O.V. TARASOV^{a3}

^aFakultät für Physik, Universität Bielefeld
D-33615 Bielefeld , Germany

^bNuclear Physics Institute of Moscow State University
119899 Moscow, Russian Federation

Abstract

A method of calculating Feynman diagrams from their small momentum expansion [1] is extended to diagrams with zero mass thresholds. We start from the asymptotic expansion in large masses [2] (applied to the case when all M_i^2 are large compared to all momenta squared). Using dimensional regularization, a finite result is obtained in terms of powers of logarithms (describing the zero-threshold singularity) times power series in the momentum squared. Surprisingly, these latter ones represent functions, which not only have the expected physical “second threshold” but have a branchcut singularity as well below threshold at a mirror position. These can be understood as pseudothresholds corresponding to solutions of the Landau equations. In the spacelike region the imaginary parts from the various contributions cancel. For the two-loop examples with one mass M , in the timelike region for $q^2 \approx M^2$ we obtain approximations of high precision. This will be of relevance in particular for the calculation of the decay $Z \rightarrow b\bar{b}$ in the $m_b = 0$ approximation.

¹ E-mail: fleischer@physik.uni-bielefeld.de

² Supported by European project Human Capital and Mobility under CHRX-CT94-0579
E-mail: smirnov@theory.npi.msu.su

³ Supported by Bundesministerium für Forschung und Technologie under PH/05-6BI93P. On leave of absence from Joint Institute for Nuclear Research, 141980 Dubna, Moscow Region, Russian Federation. Present address: IfH DESY, Zeuthen, Platanenallee 6, 15738, Germany, E-mail: tarasov@ifh.de.

1 Introduction

Once it has been observed [1] that the calculation of Feynman diagrams on their cut can be performed with high precision from their Taylor expansion coefficients, there are several advantages of this method, which make it really quite attractive: firstly, the Taylor coefficients being known, the remaining calculation of the diagram in the whole complex plane is a relatively easy task. Secondly, more important, the precision with which the coefficients can be calculated (from vacuum diagrams) is practically unlimited (e.g. 50 to 100 decimals with the multiple precision program of [3] is “standard”). This last property is of particular relevance in higher loop orders when many diagrams (of the order of 1000) contribute, namely the high precision of the Taylor coefficients suggests that in such a case the scalar amplitudes should be added on the level of their Taylor coefficients. Finally, as mentioned in [1], in the 2-loop 3-point case, in which we are mainly interested here, there occur in general 10 numerator scalar products of 4 momenta, but only 9 (internal or external) lines against which to cancel these. This causes serious problems in the evaluation of two-loop vertex Feynman diagrams which are not present if only bubble integrals are to be evaluated like in the Taylor expansion. For these reasons it appears worthwhile to develop and extend the method of Taylor expansion further to make it applicable to the various kinematical situations in the Standard Model.

The purpose of the present paper is to demonstrate an extension of the previous method [1], which can be applied for vertex diagrams with massless thresholds. In such a case the Taylor expansion of the Feynman diagrams does not exist because of logarithmic singularities at zero momenta squared. The method which we propose for this type of diagrams is a combination of using standard explicit formulae for asymptotic expansions in large masses [2] (see [4] for a short review) and the summation procedure of [1]. Thus, in the large mass limit ($M^2 \gg |q^2|$) we get power series in q^2/M^2 factorizing powers of $\ln(-q^2/M^2)$. These power series can be summed by means of Padé approximants such that the validity of this expansion is extended to large q^2/M^2 , in the spacelike region as well as in the timelike region (due to conformal mapping). Note that the general formulae for asymptotic expansions in momenta and masses [2] have been successfully applied in a number of papers [5, 6, 7]. In particular, two-loop self-energy diagrams with general masses were calculated in [6] in the region of small and large momentum, and in [7] in the case of massless thresholds and thresholds with small masses.

Our paper is organized as follows: in Sect. 2 an introductory example of a two-loop self-energy diagram is given for which the factorization of the $\ln(-q^2/M^2)$ is explicitly known. In Sect. 3 we show cases of interest for the decay $Z \rightarrow b\bar{b}$ and select typical examples for the demonstration of our method. Sect. 4 recalls the general method and demonstrates the calculation of the “naive” part. In Sects. 5 and 6 the above examples are worked out explicitly and Sect. 7 contains our conclusions.

2 An example of a two-loop self-energy diagram with zero threshold

Before turning to complicated vertex diagrams we demonstrate how the summation by Padé approximants works in a simpler case of the self-energy integral \tilde{I}_3 (see Fig. 1) with zero threshold [10], where an explicit result written in the form of the large mass expansion is known:

$$\tilde{I}_3 = \tilde{f}_0 \left(\frac{q^2}{M^2} \right) + \tilde{f}_1 \left(\frac{q^2}{M^2} \right) \ln \left(-\frac{q^2}{M^2} \right) \quad (1)$$

with

$$\tilde{f}_0 \left(\frac{q^2}{M^2} \right) = \frac{3}{2M^2} \sum_{n=0}^{\infty} \frac{n! \Gamma(\frac{3}{2})}{\Gamma(n + \frac{3}{2})(n+1)^2} \left(-\frac{q^2}{4M^2} \right)^n \quad (2)$$

$$\tilde{f}_1 \left(\frac{q^2}{M^2} \right) = -\frac{1}{2M^2} \sum_{n=0}^{\infty} \frac{n! \Gamma(\frac{3}{2})}{\Gamma(n + \frac{3}{2})(n+1)} \left(-\frac{q^2}{4M^2} \right)^n. \quad (3)$$

Summing the series for \tilde{f}_0 and \tilde{f}_1 in the “standard” manner [1], the results of Table 1. are obtained. They demonstrate that high precision numerical values can be obtained for a large range of q^2 values in this way.

3 Two-loop vertex diagrams with zero thresholds

Concerning the vertex diagrams, there are many different topologies contributing to a 3-point function in the Standard Model. For our purpose of demonstrating the method, we confine ourselves to the “planar” case with the topology shown in Fig. 2 (see “generic”). Distributing in all possible ways massive particles over the six virtual lines of this figure, one finds 22 diagrams with a zero mass threshold. Our main interest in the present study is, however, besides the development of a new method, its possible application to the calculation of the decay amplitude for $Z \rightarrow b\bar{b}$. For this process $m_b = 0$ can be considered as a good approximation and for the corresponding kinematical situation ($p_1^2 = p_2^2 = 0$) the new approach is directly applicable (see also [1]). Therefore, instead of presenting all possible 22 diagrams with zero mass thresholds, in Figs. 2 and 3 we give only those contributing to $Z \rightarrow b\bar{b}$ (with $m_b = 0$ and m_t large, neglecting quark mixing). Fig. 3 presents infrared divergent diagrams and they are merely given for completeness: *Cases* 7,8 and 9 will be considered in a separate publication. *Case* 10 is a diagram with massless particles only, and our method is of no relevance here. This diagram (and also other topologies), however, has been evaluated in [8] (see also [9]). In Figs. 2 and 3 we choose all non-zero masses to be equal ($= M$).

Typical examples which we work out here explicitly are *Case 1* and *Case 5* of Fig. 2. These have in the expansion coefficients terms of the order $1/\varepsilon$ (*Case 1*) and $1/\varepsilon$ and $1/\varepsilon^2$ (*Case 5*), respectively ($d = 4 - 2\varepsilon$). Taking into account factors of the form $\left(\frac{\mu^2}{M^2}\right)^\varepsilon$ and $\left(-\frac{\mu^2}{q^2}\right)^\varepsilon$ ($q = p_1 - p_2$), (see below) and expanding these in terms of ε , the poles in ε as well as the dependence on the scale parameter μ drop out. In the final result there remain terms factorizing $\ln(-q^2/M^2)$ and $\ln^2(-q^2/M^2)$ from the latter expansion after cancellation of the corresponding powers of ε .

4 Large mass expansion and calculation of the “naive” part

The large mass limit is obtained in the following manner: if some masses are much greater than the other masses (in our case all the small masses are zero) and all the momenta, one has [2]

$$F_\Gamma(p_1, p_2, M; \epsilon) \stackrel{M \rightarrow \infty}{\sim} \sum_\gamma F_{\Gamma/\gamma}(p_1, p_2; \epsilon) \circ \mathcal{T}_{q^\gamma} F_\gamma(q^\gamma, M; \epsilon), \quad (4)$$

F_{\dots} standing for (sub-)diagrams and reduced diagrams characterized by their index: Γ for the original diagram, γ a subdiagram ($\gamma \subset \Gamma$) and Γ/γ obtained from the original diagram by factorizing the product of scalar propagators as $\Pi_\Gamma \equiv \Pi_{\Gamma/\gamma} \Pi_\gamma$ such that more explicitly we have (l is the number of loops)

$$F_{\Gamma/\gamma} \circ \mathcal{T}_{q^\gamma} F_\gamma = \int dk_1 \cdots dk_l \Pi_{\Gamma/\gamma} \mathcal{T}_{q^\gamma} \Pi_\gamma. \quad (5)$$

Here \mathcal{T}_{\dots} is the operator of the Taylor expansion w. r. t. the set of external momenta q^γ of the subgraph γ . The summation in (4) is performed over the following subgraphs:

- each γ (it may be disconnected) contains all the lines with large masses,
- each γ is 1PI w. r. t. lines with small masses.

The (“naive”) contribution from the original diagram Γ itself is obviously always contained in the \sum_γ . In various terms of this sum the integrations of the type (5) yield in general divergent coefficients of the asymptotic expansion. These divergences are both of infrared and ultraviolet nature, the latter being due to high powers of integration momenta produced by the \mathcal{T}_{\dots} operator. Therefore (4) is to be understood in terms of some regularization for which we take dimensional regularization. This is so even if the original diagram is convergent: summing all contributions (\sum_γ) the divergent terms and those depending on the scale parameter μ (from dimensional regularization)

must cancel. This will be used below as a strong check of our calculational procedure.

In the following we will calculate the diagrams *Case 1* and *Case 5* of Fig. 2. These are typical in the sense that they have one and two zero mass thresholds, resulting in the above mentioned terms up to $1/\varepsilon$ and $1/\varepsilon^2$ in the Taylor coefficients, respectively or $\ln(-q^2/M^2)$ and $\ln^2(-q^2/M^2)$ in the final result. The three particle zero mass threshold in *Case 6* does not induce higher than $1/\varepsilon^2$ terms in the Taylor coefficients either.

The “higher” terms in the \sum_γ (i.e. all except for the naive one) can be handled in a straightforward though tedious calculation. The reason for the relative simplicity is that only factorizing massive one-loop bubble (vacuum) integrals and massless propagator type integrals occur. Results for these higher terms will be given in the following sections.

The situation is different, however, for the “naive” contribution. In this case the approach of [11] turns out to be particularly adequate. The general expansion of (any loop) scalar 3-point function with its momentum space representation $C(p_1, p_2)$ can be written as

$$C(p_1, p_2) = \sum_{l,m,n=0}^{\infty} a_{lmn} (p_1^2)^l (p_2^2)^m (p_1 p_2)^n, \quad (6)$$

where the coefficients a_{lmn} are to be determined from the given diagram. As we will show, in the cases under consideration the representation of the Taylor coefficients given in [11] yields only “genuine two-loop bubbles” but no factorizing one-loop ones. Introducing the abbreviations (see also Fig. 2) $c_1 = k_1^2 - m_1^2$, $c_2 = k_1^2 - m_2^2$, $c_3 = k_2^2 - m_3^2$, $c_4 = k_2^2 - m_4^2$ and $c_5 = k_2^2 - m_5^2$, $c_6 = (k_1 - k_2)^2 - m_6^2$, we have for the expansion coefficients

$$(i\pi^2)^2 a_{00n} = \frac{2^n}{n+1} (\mu^2)^{2\varepsilon} \int d^d k_1 d^d k_2 F_n \cdot \frac{1}{c_1 c_2 c_3 c_4 c_5 c_6}, \quad (7)$$

where μ is the scale parameter of dimensional regularization.

In general the vertex diagram depends on three external momenta squared (see 6), each of which is an independent expansion variable. Putting $p_1^2 = p_2^2 = 0$ the corresponding summation indices are also zero. In (7) F_n is given by

$$F_n = \sum_{\nu, \nu', \mu'} a_{\nu\nu'}^{n\mu'} \frac{(k_1^2)^{n-(\nu+\nu')+\mu'}}{c_1^{n-\nu} c_2^{n-\nu'}} \frac{(k_2^2)^{\mu'}}{c_3^\nu c_4^{\nu'}} \frac{1}{2^{\nu+\nu'-2\mu'}} \left\{ (k_1^2 + k_2^2 - m_6^2)^{\nu+\nu'-2\mu'} - \sum_{\alpha=1, \text{odd}}^{\nu+\nu'-2\mu'} (k_1^2 + k_2^2 - m_6^2)^{\nu+\nu'-2\mu'-\alpha} (2k_1 k_2)^{\alpha-1} \cdot c_6 \right\}, \quad (8)$$

the coefficients $a_{\nu\nu'}^{n\mu'}$ being known explicitly for arbitrary d [11]. We see that due to cancellation of c_6 in the above sum over α this contribution contains only factorizing one-loop terms which vanish for the above mass combinations

in dimensional regularization. Thus it remains to calculate the "genuine two-loop" contributions.

In Case 1 ($m_6 = M$) we write ($\lambda = \nu + \nu' - 2\mu'$)

$$(k_2^2)^{\mu'} (k_1^2 + k_2^2 - M^2)^\lambda = \sum_{\beta=0}^{\lambda} \sum_{\gamma=0}^{\mu'} \binom{\lambda}{\beta} \binom{\mu'}{\gamma} (M^2)^{\mu'-\gamma} (k_1^2)^{\lambda-\beta} c_3^{\beta+\gamma}$$

and obtain

$$\begin{aligned} a_{00n} &= \frac{2^n}{n+1} \sum_{\nu, \nu', \mu'} a_{\nu\nu'}^{n\mu'} \frac{1}{2^\lambda} \sum_{\beta=0}^{\lambda} \sum_{\gamma=0}^{\mu'} \binom{\lambda}{\beta} \binom{\mu'}{\gamma} \\ &\times (M^2)^{\mu'-\gamma} \frac{(\mu^2)^{2\varepsilon}}{(i\pi^2)^2} \int d^d k_1 d^d k_2 \frac{1}{(k_1^2)^{\nu_1} c_3^{\nu_2} c_6} \end{aligned} \quad (9)$$

with $\nu_1 = n - (\nu + \nu') + \mu' + \beta + 2$ and $\nu_2 = (\nu + \nu') - \beta - \gamma + 3$. The two-loop bubble integrals can be evaluated explicitly:

$$\begin{aligned} &\frac{1}{(i\pi^2)^2} \int d^d k_1 d^d k_2 \frac{1}{(k_1^2)^{\nu_1} c_3^{\nu_2} c_6} \\ &= (-1)^{(\nu_1 + \nu_2 + 1)} \frac{\Gamma(\nu_1 + \nu_2 + 1 - d) \Gamma(\frac{d}{2} - \nu_1) \Gamma(\nu_1 + \nu_2 - \frac{d}{2}) \Gamma(\nu_1 + 1 - \frac{d}{2})}{\Gamma(\nu_2) \Gamma(\frac{d}{2}) \Gamma(2\nu_1 + \nu_2 + 1 - d) (M^2)^{(\nu_1 + \nu_2 + 1 - d)}}. \end{aligned}$$

Expanding in ε , a divergent $\frac{1}{\varepsilon}$ -term is obtained, which in this case comes from the infrared divergence of the above integral.

Similarly as above we calculate the "naive" part for Case 5: with

$$(k_2^2)^{\mu'} (k_1^2 + k_2^2 - M^2)^\lambda = \sum_{\beta=0}^{\lambda} \sum_{\gamma=0}^{\beta} \binom{\lambda}{\beta} \binom{\beta}{\gamma} (-M^2)^{\beta-\gamma} (k_1^2)^{\lambda-\beta} (k_2^2)^{\mu'+\gamma}$$

we have

$$\begin{aligned} a_{00n} &= \frac{2^n}{n+1} \sum_{\nu, \nu', \mu'} a_{\nu\nu'}^{n\mu'} \frac{1}{2^\lambda} \sum_{\beta=0}^{\lambda} \sum_{\gamma=0}^{\beta} \binom{\lambda}{\beta} \binom{\beta}{\gamma} \\ &\times (-M^2)^{\beta-\gamma} \frac{(\mu^2)^{2\varepsilon}}{(i\pi^2)^2} \int d^d k_1 d^d k_2 \frac{1}{(k_1^2)^{\nu_1} c_3^{(\nu_2-1)} c_5 c_6} \end{aligned} \quad (10)$$

with ν_1 and ν_2 as above. The situation is now somewhat more complicated due to the fact that $m_3 \neq m_5$ and the following partial fraction decomposition needs to be performed ($p = \nu_2 - 2$, $m_3 = 0$ and $m_5 = M$):

$$\frac{1}{c_3^{p+1} c_5} = - \sum_{i=0}^p \frac{1}{(M^2)^{p+1-i} c_3^{i+1}} + \frac{1}{(M^2)^{p+1} c_5},$$

yielding the two-loop bubble Integrals

$$\frac{1}{(i\pi^2)^2} \int d^d k_1 d^d k_2 \frac{1}{(k_1^2)^{\nu_1} c_3^{i+1} c_6} =$$

$$(-1)^{(\nu_1+i)} \frac{\Gamma(\nu_1 + i + 2 - d) \Gamma(\frac{d}{2} - i - 1) \Gamma(\nu_1 + i + 1 - \frac{d}{2}) \Gamma(\frac{d}{2} - \nu_1)}{\Gamma(\nu_1) \Gamma(\frac{d}{2}) \Gamma(i + 1) (M^2)^{(\nu_1+i+2-d)}}$$

and

$$\frac{1}{(i\pi^2)^2} \int d^d k_1 d^d k_2 \frac{1}{(k_1^2)^{\nu_1} c_5 c_6} =$$

$$(-1)^{\nu_1} \frac{\Gamma(\nu_1 + 2 - d) \Gamma(\frac{d}{2} - \nu_1) \Gamma^2(\nu_1 + 1 - \frac{d}{2})}{\Gamma(\frac{d}{2}) \Gamma(2\nu_1 + 2 - d) (M^2)^{(\nu_1+2-d)}}.$$

Expanding in ε , in this case $\frac{1}{\varepsilon^2}$ -terms occur.

5 Threshold singularity of the type $\ln(-q^2/M^2)$ (*Case 1*)

According to Fig. 2 there is only one subdiagram γ which contains all four massive lines, namely the box. Accordingly the only contribution with $\gamma \neq \Gamma$ reads

$$(\mu^2)^{2\varepsilon} \int \frac{d^d k_1}{k_1^2 (q - k_1)^2} \int \frac{d^d k_2}{(k_2^2 - M^2)} \times$$

$$\times \mathcal{T}_{p_1, q, k_1} \frac{1}{[(k_1 - k_2)^2 - M^2][(q + k_2)^2 - M^2][(p_1 - k_2)^2 - M^2]}. \quad (11)$$

Here the external momenta for the box subgraph are besides p_1 and q also the loop momentum k_1 . Note that, for the contributions of each subgraph γ in (4) one can choose loop momenta in an appropriate way. For example, in (11) the rooting of the loop momenta is different from the “naive” contribution (observe also below similar rerooting in *Case 5*).

The evaluation of (11) results in products of one-loop massive bubble integrals with monomials in the numerator and one-loop propagator-type massless integrals, the latter yielding the factor $(-1/q^2)^\varepsilon$. Explicitly we obtain

$$\frac{1}{(4\pi)^d} \frac{1}{M^4} \left(\frac{\mu^2}{M^2} \right)^\varepsilon \left(-\frac{\mu^2}{q^2} \right)^\varepsilon \sum_{n=0}^{\infty} c_n^{(2)}(\varepsilon) (q^2/M^2)^n, \quad (12)$$

where

$$c_n^{(2)}(\varepsilon) = \sum_{\substack{i_1, i_2, n_3 \geq 0, \\ i_1 + i_2 + n_3 \leq 2n}} \sum_{\substack{j_3 \geq 0 \\ \text{even}}}^{(n_3, -2)} (-1)^{(i_1 + i_2 + n_3)/2} \frac{(n - (i_1 + i_2 - n_3)/2)!}{(n - (i_1 + i_2 + n_3)/2)!}$$

$$\begin{aligned} & \times \frac{i_1!i_2!\theta(i_1+i_2-j_3)\theta(i_1-i_2+j_3)\theta(-i_1+i_2+j_3)}{((n_3-j_3)/2)!((i_1+i_2-j_3)/2)!((i_1-i_2+j_3)/2)!((-i_1+i_2+j_3)/2)!} \\ & \quad \times \frac{\Gamma(\epsilon)\Gamma(1-\epsilon)\Gamma((i_1+i_2-j_3)/2+1-\epsilon)}{\Gamma((i_1+i_2-j_3)/2+2-2\epsilon)} \\ & \quad \times C(n+(i_1+i_2+n_3)/2+4; (i_1+i_2+n_3)/2) \end{aligned} \quad (13)$$

and

$$C(r, s) = \Gamma\left(r - s - \frac{d}{2}\right) / \Gamma(r). \quad (14)$$

The ε -poles in this case come from ultraviolet divergences. Adding the naive and the above contribution yields (up to a factor $(1/16\pi^2)^2$)

$$\begin{aligned} F_\Gamma(q^2, M^2) &= \frac{1}{M^4} \left\{ \sum_{n=0}^{\infty} f_{0n}(q^2/M^2)^n + \sum_{n=0}^{\infty} f_{1n}(q^2/M^2)^n \ln(-q^2/M^2) \right\} \\ &\equiv \frac{1}{M^4} \left\{ f_0(q^2/M^2) + f_1(q^2/M^2) \ln(-q^2/M^2) \right\}, \end{aligned} \quad (15)$$

i.e. all ε -poles and the scale parameter μ have cancelled, which at the same time serves as a helpful check of the correctness of the calculation. Evaluating the complicated coefficients and summing all contributions was performed with FORM [12]. For the expansion coefficients of f_1 we found by inspection the following recurrence relation:

$$\begin{aligned} & 8(2n+5)(2n+7)(2n+9)(n+4) f_{1,n+3} = \\ & - 4(2n+5)(2n+7)(n+4)^2 f_{1,n+2} \\ & + 2(2n+5)(n+3)(n+2)^2 f_{1,n+1} + (n+3)(n+2)^3 f_{1,n}, \end{aligned} \quad (16)$$

from which we obtain:

$$f_{1,n} = \frac{\Gamma(n+2)\Gamma(\frac{5}{2})}{6(-4)^n\Gamma(n+\frac{5}{2})} \sum_{j=0}^n \frac{1+2(-1)^j}{(j+1)^2}. \quad (17)$$

This explicit form allows to sum the series for f_1 , yielding the following integral representation:

$$f_1 = \sum_{n=0}^{\infty} \left(-\frac{q^2}{M^2}\right)^n f_{1,n} = \frac{M^2}{q^2} \int_0^1 \ln zdz \left[\phi\left(z, \frac{q^2}{M^2}\right) - 2\phi\left(-z, \frac{q^2}{M^2}\right) \right] \quad (18)$$

where

$$\phi(z, x) = \frac{4 \arcsin(\sqrt{zx/4})}{(1-z)\sqrt{zx(4+zx)}}. \quad (19)$$

An interesting feature of this representation is that two thresholds, one at $q^2 = 4M^2$ and another at $q^2 = -4M^2$ can immediately be read off. There ought to be, however, only one threshold at $q^2 = 4M^2$. Indeed it turns out that f_0 has a singularity at $q^2 = -4M^2$ as well and that for $q^2 < -4M^2$ the imaginary part of $f_1 \ln(-q^2/M^2)$ and f_0 cancel.

Note that the position of the “mirror” threshold of the functions f_0 and f_1 exactly corresponds to a pseudothreshold of the given Feynman diagram which is a solution of the Landau equations (see e.g. [13]). In fact solving these, we obtain for $m_1 = m_2 = 0$ the pseudothreshold $q^2 = -(m_5 + m_6)^2$.⁴ An even simpler case is the corresponding one-loop vertex with a massive line connecting two massless ones. This graph is proportional to ($x=q^2/M^2$)

$$Li_2(1+x) - \zeta(2) = -Li_2(-x) - \ln(1+x)\ln(-x), \quad (20)$$

where in the second form of writing the logarithmic singularity at $x=0$ has been isolated and now again the pseudothreshold singularity at $x=-1$ appears in the separate terms. For two-loop self-energy diagrams one obtains by inspection corresponding results from Refs. [7] and [14]. At this point it is interesting to note that the self-energy diagram \tilde{I}_3 , dealt with in Sect.2, has no pseudothreshold, i.e. no such solution of the Landau equations exists.

We have found, however, a closed form as in (18) only for f_1 and not for f_0 . Therefore, to demonstrate the above statement, we have to rely on our numerical approach. Results for *Case 1* are given in Tables 2 to 4 (in all tables the results are given up to a factor $\frac{1}{(16\pi^2)^2 M^4}$).

Table 2 gives results for spacelike q^2 . For $0 > q^2 \geq -4M^2$ we achieve fast convergence, calculating the indicated Padé approximants, taking into account Taylor coefficients up to $n=30$. Of course the integral is real in this domain and agrees excellently with the Monte Carlo control calculation (five dimensional integration over Feynman parameters with an estimated relative error $< 10^{-4}$).

For $q^2 < -4M^2$ we first performed a conformal mapping in terms of an “ ω -transform” [1] before using Padé approximants to sum the series for f_0 and f_1 . This is of course always necessary if one wants to calculate a function on a cut. As a result we obtain in the above domain small imaginary parts, which are due to insufficient cancellation of the two imaginary parts. It is seen, however, that these become quickly small with increasing order of the approximants. The situation becomes even more amazing if one looks at the imaginary parts of f_0 and f_1 separately: they do increase with q^2 relative to their real parts as is demonstrated in Table 4! Nevertheless, in this manner we obtain even for large negative values like $q^2/M^2 = -50$ an accuracy of at least 3 decimals as is also confirmed by the MC control calculation.

Table 3 gives our results in the timelike region. The analytic continuation of the logarithm requires in this case to write

$$\ln(-q^2/M^2) = \ln |q^2/M^2| - i\pi \quad (21)$$

⁴We are grateful to J.B. Tausk who has drawn our attention to this property and provided several examples, including the following one.

so that an imaginary part is obtained for $q^2 > 0$. Table 3 gives only results above the second threshold since below the convergence is even better: at $q^2 = M^2$ we obtain a precision of 9 decimals with merely 9 coefficients ([4/4]). A precision of at least 3 decimals is achieved both for the real and imaginary part up to $q^2/M^2=50$. This can be concluded from the convergence properties of the approximants.

6 Threshold singularity of the type

$\ln^2(-q^2/M^2)$ (Case 5)

There are two massless cuts so that we shall have the double logarithm in the expansion. The set of subgraphs in this case is given by $\gamma_1 = \Gamma$ and the higher terms with $\gamma \neq \Gamma$: $\gamma_2 = \{3456\}$, $\gamma_3 = \{1256\}$, and $\gamma_4 = \{56\}$. Note that γ_3 and γ_4 are disconnected. The subgraph γ_1 was discussed in Sect. 4. In terms of integrals of the form (5) we have

for γ_2

$$\begin{aligned} & (\mu^2)^{2\varepsilon} \int d^d k_1 \frac{1}{k_1^2 (q - k_1)^2} \\ & \times \int d^d k_2 \frac{1}{k_2^2} \mathcal{T}_{p_1, q, k_1} \frac{1}{((p_1 + k_2)^2 - M^2)((k_1 - k_2)^2 - M^2)(q - k_2)^2}, \end{aligned} \quad (22)$$

for γ_3

$$\begin{aligned} & (\mu^2)^{2\varepsilon} \int d^d k_2 \frac{1}{k_2^2 (q - k_2)^2} \mathcal{T}_{p_1, k_2} \frac{1}{(p_1 + k_2)^2 - M^2} \\ & \times \int d^d k_1 \frac{1}{k_1^2} \mathcal{T}_{q, k_2} \frac{1}{((k_1 - k_2)^2 - M^2)(q - k_1)^2} \end{aligned} \quad (23)$$

and finally for γ_4

$$\begin{aligned} & (\mu^2)^{2\varepsilon} \int d^d k_2 \frac{1}{k_2^2 (q - k_2)^2} \mathcal{T}_{p_1, k_2} \frac{1}{(p_1 + k_2)^2 - M^2} \\ & \times \int d^d k_1 \frac{1}{k_1^2 (q - k_1)^2} \mathcal{T}_{k_1, k_2} \frac{1}{(k_1 - k_2)^2 - M^2}. \end{aligned} \quad (24)$$

The results for these three integrals look as follows. The subgraph γ_2 yields

$$\frac{1}{(4\pi)^d} \frac{1}{M^4} \left(\frac{\mu^2}{M^2} \right)^\varepsilon \left(-\frac{\mu^2}{q^2} \right)^\varepsilon \sum_{n=0}^{\infty} c_n^{(2)}(\varepsilon) (q^2/M^2)^n, \quad (25)$$

where

$$c_n^{(2)}(\varepsilon) = \sum_{\substack{i_1, i_2, n_3 \geq 0, \\ i_1 + i_2 + n_3 \leq 2n}} \sum_{\substack{\text{even } i_1 + i_2 + n_3 \\ j_3 \geq 0}}^{(n_3, -2)} (-1)^{(i_1 + i_2 + n_3)/2} \frac{(n - (i_1 + i_2 - n_3)/2)!}{(n - (i_1 + i_2 + n_3)/2)!}$$

$$\begin{aligned}
& \times \frac{i_1!i_2!\theta(i_1+i_2-j_3)\theta(i_1-i_2+j_3)\theta(-i_1+i_2+j_3)}{((n_3-j_3)/2)!((i_1+i_2-j_3)/2)!((i_1-i_2+j_3)/2)!((-i_1+i_2+j_3)/2)!} \\
& \quad \times \frac{\Gamma(\epsilon)\Gamma(1-\epsilon)\Gamma((i_1+i_2-j_3)/2+1-\epsilon)}{\Gamma((i_1+i_2-j_3)/2+2-2\epsilon)} \\
& \quad \times C(2+i_1+i_2, 2+n-(i_1+i_2-n_3)/2; (i_1+i_2+n_3)/2), \quad (26)
\end{aligned}$$

and

$$C(r_1, r_2; s) = \frac{\Gamma(r_1+r_2-s-\frac{d}{2})\Gamma(s-r_2+\frac{d}{2})}{\Gamma(r_1)\Gamma(s+\frac{d}{2})}. \quad (27)$$

Note that this expression is obtained from the corresponding contribution of the non-naive part (13) for our first diagram by the change

$$\begin{aligned}
& C(2+i_1+i_2, 2+n-(i_1+i_2-n_3)/2; (i_1+i_2+n_3)/2) \\
& \rightarrow C(n+(i_1+i_2+n_3)/2+4; (i_1+i_2+n_3)/2).
\end{aligned}$$

The contribution from γ_3 takes the following explicit form:

$$\frac{1}{(4\pi)^d} \frac{1}{M^4} \left(\frac{\mu^2}{M^2}\right)^\epsilon \left(-\frac{\mu^2}{q^2}\right)^\epsilon \sum_{n=0}^{\infty} c_n^{(3)}(\epsilon) (q^2/M^2)^n, \quad (28)$$

where

$$\begin{aligned}
c_n^{(3)}(\epsilon) = (-1)^n & \sum_{\substack{i_1 \geq 0 \\ i_1 - (n_1 - j_1)/2 \leq n}} \sum_{n_1=0}^{i_1} \sum_{j_1 \geq 0}^{(n_1, -2)} (-1)^{i_1+j_1} \frac{i_1!}{(i_1-n_1)!((n_1-j_1)/2)!} \\
& \times \frac{\Gamma(2-\frac{d}{2})\Gamma(\frac{d}{2}-1)\Gamma(n-i_1+(n_1-j_1)/2+\frac{d}{2}-1)}{\Gamma(n-i_1+(n_1-j_1)/2+\frac{d}{2})} \\
& \quad \times C(j_1+1, i_1+2; (n_1+j_1)/2). \quad (29)
\end{aligned}$$

Finally, for γ_4 we obtain

$$\frac{1}{(4\pi)^d} \frac{1}{M^4} \left(-\frac{\mu^2}{q^2}\right)^{2\epsilon} \sum_{n=0}^{\infty} c_n^{(4)}(\epsilon) (q^2/M^2)^n, \quad (30)$$

with

$$c_n^{(4)}(\epsilon) = (-1)^n (\Gamma(2-\frac{d}{2})\Gamma(\frac{d}{2}-1))^2 \sum_{j=0}^n \frac{\Gamma(j+\frac{d}{2}-1)\Gamma(n-j+\frac{d}{2}-1)}{\Gamma(j+d-2)\Gamma(n-j+d-2)}. \quad (31)$$

After summing up all four contributions we see that the double and single poles in ϵ cancel as well as the scale parameter μ , with the result

$$\begin{aligned}
F_\Gamma(q^2, M^2) &= \frac{1}{M^4} \sum_{n=0}^{\infty} \sum_{j=0}^2 f_{jn}(q^2/M^2)^n \ln^j(-q^2/M^2) \\
&\equiv \frac{1}{M^4} \left\{ f_0(q^2/M^2) + f_1(q^2/M^2) \ln(-q^2/M^2) + f_2(q^2/M^2) \ln^2(-q^2/M^2) \right\}, \quad (32)
\end{aligned}$$

where the f_{jn} are now obtained in terms of rational numbers and a $\zeta(2)$ contained in f_{0n} .

The next surprise is that $f_2(x)$ can be summed analytically, yielding ($x = q^2/M^2$)

$$\begin{aligned} f_2(x) &= \ln^2(1+x)/x^2 && \text{for } x \geq -1, \\ &= (\ln |1+x| - i\pi)^2/x^2 && \text{for } x < -1. \end{aligned} \quad (33)$$

Thus, as in *Case 1*, we have to Padé approximate f_0 and f_1 only. The $\zeta(2)$ term in f_0 can in principle also be summed, i.e.

$$f_0(x) = \tilde{f}_0(x) + 2\zeta(2)f_2(x), \quad (34)$$

with $\tilde{f}_0(x)$ having only rational numbers as expansion coefficients. This splitting does, however, worsen the convergence properties of the series for f_0 and therefore has no practical meaning. Apart from that the situation is similar as in *Case 1*, i.e. f_0 has two thresholds starting at $q^2 = \pm M^2$, respectively (indeed solving the Landau equations with $m_1 = m_2 = m_3 = m_4 = 0$ one obtains the additional pseudothreshold $q^2 = -m_5^2$). The function f_1 , however, is real for timelike q^2 . In the spacelike region the cancellation between the imaginary parts has now to take place between three complex functions. This is shown in Table 5, but apparently this cancellation is not as perfect as in *Case 1*. This is due to a relatively bad convergence of the Padé's for f_0 (with 30 coefficients) while the convergence properties of f_1 are much better and f_2 is anyway given analytically. Fortunately the convergence of f_0 is much better in the timelike region (see Table 6) so that up to $q^2 = 10M^2$ the achieved precision is at least 3 decimals. Close to the second threshold at $q^2 = M^2$ the convergence is indeed excellent. It should be noted that for the physical application we have in mind, i.e. $Z \rightarrow b\bar{b}$, this is just the case of interest. It is worthwhile to note the sharp increase for low q^2 , in particular in the timelike region, due to $\ln^2(-q^2/M^2)$.

7 Conclusions

We have presented a modification of the method of [1] for the case when massless thresholds are involved. To do this, the starting point was the asymptotic large mass expansion, rather than the Taylor expansion in the external momenta. Using the explicit formulae for the coefficients of this expansion we obtained a finite sum of powers of the logarithm of the external momenta times power series in q^2/M^2 and then applied the technique of conformal mapping and summation by Padé approximants to each of these series separately.

We have shown that this new strategy enables us to obtain high precision numerical values in the domain of physical interest including the region beyond the second threshold in spite of the fact that the initial Feynman diagrams have their first threshold at the origin of the complex plane. Below the second threshold, in a certain domain around $q^2 = 0$, the functions factorizing powers

of $\ln(-q^2/M^2)$ can in general be assumed to be analytic so that even without Padé approximants their power series converge. At the second threshold with definiteness one can only say that at least one of them must have a cut starting. This is confirmed by our calculation, i.e. the application of conformal mapping and Padé approximants (recall the observation that in *Case 5* f_1 is real for timelike q^2). The occurrence of “ghost thresholds” appears to be related to pseudothresholds obtained from the Landau equations.

Acknowledgement

We are grateful to J.B.Tausk for helpful comments concerning the “ghost thresholds”. O.T. gratefully acknowledges financial support by the BMBF, V.S. from the European Community under the project Human Capital and Mobility. J.F. thankfully acknowledges financial support by the DFG for travel expences to Aspen, where part of this work was performed and to DESY, Zeuthen to finish it.

References

- [1] J. Fleischer and O.V. Tarasov, *Z. Phys.*, C 64 (1994) 413.
- [2] S.G. Gorishny, preprints JINR E2–86–176, E2–86–177 (Dubna 1986); *Nucl. Phys.* B319 (1989) 633; K.G. Chetyrkin, *Teor. Mat. Fiz.* 75 (1988) 26; 76 (1988) 207; V.A. Smirnov, *Commun. Math. Phys.* 134 (1990) 109; K.G. Chetyrkin, preprint MPI-PAE/PTh 13/91 (Munich, 1991); V.A. Smirnov, *Renormalization and asymptotic expansions* (Birkhäuser, Basel, 1991).
- [3] D.H. Bailey, *ACM Transactions on Mathematical Software*, 19 (1993) 288.
- [4] V.A. Smirnov, *Mod. Phys. Lett. A* 10 (1995) 1485.
- [5] K.G. Chetyrkin, *Phys. Lett.* B303 (1993) 169; K.G. Chetyrkin and A. Kwiatkowski, *Phys. Lett.* B305 (1993) 285, B319 (1993) 307; K.G. Chetyrkin and O.V. Tarasov, *Phys. Lett.* B327 (1994) 114; S.A. Larin, T. van Ritbergen and J.A.M. Vermaseren, *Phys. Lett.* B320 (1994) 159; *Nucl. Phys.* B 438 (1995) 278; K.G. Chetyrkin, J.H. Kühn and M. Steinhauser, preprint TTP95-13.
- [6] A.I. Davydychev and J.B. Tausk, *Nucl. Phys.* B 397 (1993) 123; A.I. Davydychev, V.A. Smirnov and J.B. Tausk, *Nucl. Phys.* B 410 (1993) 325.
- [7] F.A. Berends, A.I. Davydychev, V.A. Smirnov and J.B. Tausk, *Nucl. Phys.* B 439 (1995) 536; F.A. Berends, A.I. Davydychev and V.A. Smirnov, preprint INLO–PUB–21/95 (hep-ph/9602396).
- [8] R.J. Gonsalves, *Phys. Rev.* D 28 (1983) 1542.
- [9] W.L. van Neerven, *Nucl.Phys.* B268 (1986) 453; G. Kramer and B. Lampe, *J.Math.Phys.* 28 (1987) 945.

- [10] D. J. Broadhurst, J. Fleischer and O.V. Tarasov, *Z. Phys. C* 60 (1993) 287.
- [11] J.Fleischer and O.V.Tarasov, in proceedings of the ZiF conference on *Computer Algebra in Science and Engineering*, Bielefeld, 28-31 August 1994, World Scientific 1995, J. Fleischer, J. Grabmeier, F.W.Hehl and W.Küchlin editors.
- [12] J.A.M. Vermaseren: Symbolic manipulation with FORM, Amsterdam, Computer Algebra Nederland, 1991.
- [13] C.Itzykson and J.-B. Zuber, “Quantum Field Heory”, McGraw-Hill Book Company, 1980.
- [14] R. Scharf and J.B. Tausk, *Nucl. Phys. B* 412 (1994) 523.

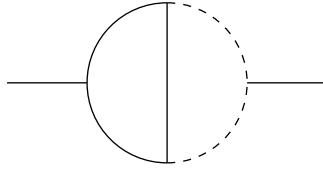
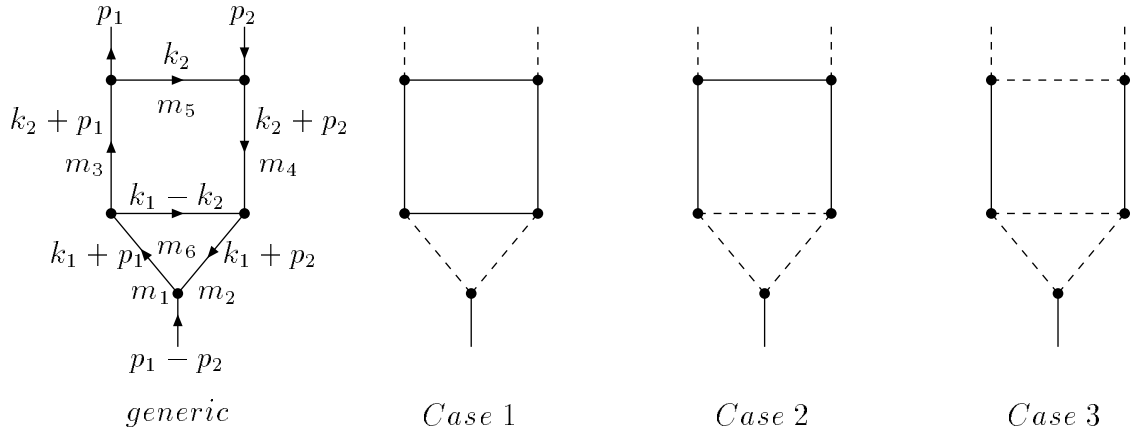
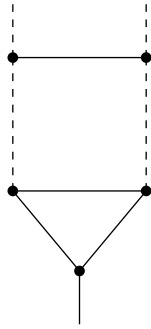
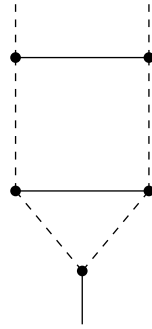


Figure 1: Self-energy integral \tilde{I}_3 ; dashed lines are massless and solid lines massive.

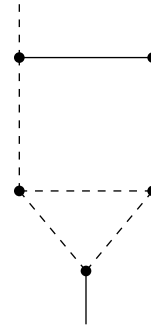




Case 4

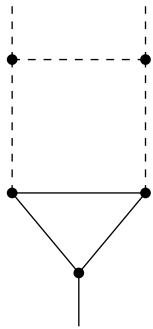


Case 5

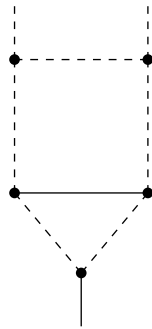


Case 6

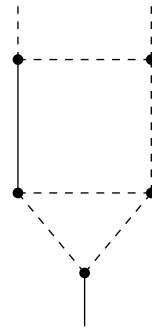
Figure 2: Planar diagrams with zero thresholds occurring in $Z \rightarrow b\bar{b}$.



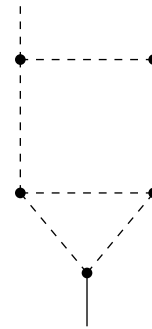
Case 7



Case 8



Case 9



Case 10

Figure 3: On-shell infrared divergent planar diagrams with zero thresholds.

Table 1. Results for the propagator diagram \tilde{I}_3

q^2/M^2	[4/4]		[7/7]		[10/10]	
	Re	Im	Re	Im	Re	Im
-1000.0	0.0068		0.007073		0.007070	
-800.0	0.0085		0.008805		-0.008804	
-400.0	0.0171		0.017322		0.01732185	
-200.0	0.0336		0.0337253		0.0337253247	
-100.0	0.0648		0.0645918		0.06459180556	
5.0	-1.128717	2.10428	-1.128713623	2.10428193574	-1.12871362356851	2.1042819357340
100.0	-0.0778	0.0071	-0.077798	0.0777	-0.0777996	0.0776864
200.0	-0.037	0.0018	-0.037924	0.00216	-0.037925	0.0021494
400.0	-0.017	0.002	-0.01866	0.0006	-0.018619	0.00059
800.0	-0.0097	0.003	-0.00917	0.00005	-0.009197	0.00003
1000.0	-0.009	0.003	-0.0072	-0.00001	-0.00734	0.0001

Table 2. Results for spacelike q^2 (Case 1)

q^2/M^2	[9/9]		[12/12]		[15/15]		MC
	Re	Im	Re	Im	Re	Im	
-2.0	0.25432052571		0.25432052571		0.25432052571		0.254320
-3.0	0.198819762		0.19881976261		0.19881976261		0.198819
-4.0	0.1633356		0.16333626		0.16333623		0.163336
-5.0	0.138397	-0.000002	0.138396	-0.00000009	0.13839601	-0.000000001	0.138396
-10.0	0.07673	-0.00003	0.07672	0.000002	0.076712	0.0000001	0.076711
-15.0	0.0516	0.0001	0.05156	0.000008	0.051582	-0.000001	0.051581
-20.0	0.0380	0.0002	0.03804	-0.00006	0.03809	-0.0000009	0.038089
-25.0	0.0294	0.0002	0.0298	-0.0002	0.02977	0.000006	0.029761
-30.0	0.0237	0.00002	0.0243	-0.0002	0.02416	0.00002	0.024157
-35.0	0.0196	-0.0002	0.0205	-0.0003	0.0202	0.00003	0.020156
-40.0	0.017	-0.0003	0.0177	-0.0002	0.0172	0.00004	0.017173
-50.0	0.013	-0.0006	0.014	-0.00006	0.0130	0.00005	0.013056

Table 3. Results for timelike q^2 (Case 1)

q^2/M^2	[9/9]		[12/12]		[15/15]	
	Re	Im	Re	Im	Re	Im
4.0	-0.163701	1.4353349	-0.163701674	1.43533447	-0.163701678	1.435334465
4.5	-0.690826	0.7787581	-0.690827345	0.77875789	-0.690827338	0.778757876
5.0	-0.697966	0.496177	-0.697964140	0.49617416	-0.697964136	0.496174195
10.0	-0.27958	-0.05286	-0.279528	-0.0528880	-0.2795301	-0.0528888
15.0	-0.13757	-0.0710	-0.137530	-0.070805	-0.137515	-0.070811
20.0	-0.0803	-0.0608	-0.08063	-0.06040	-0.08060	-0.06036
25.0	-0.0516	-0.0498	-0.05249	-0.04969	-0.05250	-0.04958
30.0	-0.03535	-0.0409	-0.03656	-0.04119	-0.03666	-0.04103
35.0	-0.0253	-0.0337	-0.0267	-0.0346	-0.0269	-0.03445
40.0	-0.019	-0.028	-0.0201	-0.0295	-0.0205	-0.0294
50.0	-0.011	-0.020	-0.0122	-0.0222	-0.0129	-0.0222

Table 4. Functions f_0 and f_1 for spacelike q^2 (Case 1)

q^2/M^2	f_0		f_1	
	Re	Im	Re	Im
-10.0	0.3089986	0.2379654	-0.10088085	-0.10334701
-20.0	0.11738	0.21435	-0.026466	-0.07155209
-30.0	0.05141	0.1635	-0.0080116	-0.048058
-40.0	0.0235	0.1274	-0.001715	-0.03453
-50.0	0.00981	0.1024	0.000813	-0.02615

Table 5. Results for spacelike q^2 (Case 5)

q^2/M^2	[9/9]		[12/12]		[15/15]		MC
	Re	Im	Re	Im	Re	Im	
-0.50	3.19126		3.191566		3.1912565		3.1912
-0.75	2.32		2.303		2.2999		2.2992
-1.0	1.80		1.797		1.7955		1.7946
-2.0	0.930	-0.0096	0.936	0.00046	0.9373	0.00011	0.9372
-3.0	0.657	0.024	0.626	-0.0015	0.6205	-0.0018	0.6193
-4.0	0.387	0.11	0.435	0.04	0.4470	0.02	0.4547
-5.0	0.14	-0.02	0.30	-0.07	0.3509	-0.05	0.3549

Table 6. Results for timelike q^2 (Case 5)

q^2/M^2	[9/9]		[12/12]		[15/15]	
	Re	Im	Re	Im	Re	Im
0.05	+2.948516245	20.938528	+2.948516245	20.938528	+2.948516245	20.938528
0.1	-1.108116127	16.04132127	-1.108116127	16.04132127	-1.108116127	16.04132127
0.5	-4.820692281	5.066080015	-4.820692281	5.066080015	-4.820692281	5.066080015
1.0	-3.89013	1.675498	-3.890154	1.67549787	-3.890156	1.67549788
1.5	-2.9046	0.4296	-2.904588	0.42979	-2.904581	0.429778
2.0	-2.1827	-0.0694	-2.18294	-0.06976	-2.182981	-0.069728
3.0	-1.335	-0.366	-1.3334	-0.3655	-1.33309	-0.3656
4.0	-0.890	-0.404	-0.8910	-0.400	-0.8907	-0.3994
5.0	-0.629	-0.380	-0.634	-0.376	-0.6347	-0.3748
6.0	-0.46	-0.340	-0.471	-0.339	-0.474	-0.338
7.0	-0.35	-0.30	-0.362	-0.301	-0.366	-0.302
8.0	-0.27	-0.26	-0.286	-0.266	-0.290	-0.269
9.0	-0.22	-0.23	-0.231	-0.235	-0.235	-0.240
10.0	-0.18	-0.19	-0.191	-0.208	-0.194	-0.215